CRITICAL FEATURES CONTROLLING THE EVOLUTION OF THE BEJA LAYERED GABBROIC SEQUENCE; IMPLICATIONS TO ORE-FORMING PROCESSES

Jesus, A.P., Munhá, J., Mateus, A.

Departamento de Geologia, Centro de Geologia and CREMINER, Faculdade de Ciências, Universidade de Lisboa, Ed. C6, Piso 4, Campo Grande, 1749-016 Lisboa, Portugal

Resumo: O domínio NW da Sequência Gabróica Bandada (SGB) inclui cinco Séries, quatro delas (SB I, II e ODV I, II) relacionadas com mineralizações de óxidos Fe-Ti-V. Dados petrográficos e de química mineral foram avaliados com o propósito de analisar a variação de parâmetros intensivos ao longo da evolução deste domínio da SGB. Os principais resultados obtidos são: 1) SB I cristalizou a partir de um magma oxidado primitivo, possivelmente o magma parental da SGB; 2) a transição SB I - SB II é marcada por queda abrupta de fO_2; 3) o menor ΔfO_2 (FMQ) e a maior T de fecho são obtidos para os cumulados enriquecidos em óxidos na base de ODV I; 4) regista-se recuperação fO_2 após o evento mineralizante; e 5) as características mais primitivas de ODV II traduzem novos influxos de magmas primitivos e/ou mistura com o magma residual (evoluído) envolvido na cristalização de ODV I.

Abstract: The NW domain of the Layered Gabbroic Sequence (LGS) includes five Series, four of them (SB I, II and ODV I, II) closely related to Fe-Ti-V oxide mineralizations. Petrographic and mineral chemistry data was gathered in order to access the variation of intensive parameters throughout the evolution of this LGS domain. The main results are as follows: 1) SB I crystallized from an oxidized primitive magma, possibly the LGS parental magma; 2) SB I - SB II transition is marked by a sudden drop of fO_2; 3) the lowest ΔfO_2 (FMQ) and the highest closure T are observed for the oxide-rich cumulates occurring at the base of ODV I; 4) fO_2 seems to have recovered to "normal levels ($\Delta fO_2 = 0 \pm 1$)" after the oxide ore-forming event; and 5) more primitive features of ODV II rocks reflect new magma influxes into the chamber and/or mixing with residual (evolved) magma forming ODV I.

1. Introduction and previous work

The Beja Igneous Complex (BIC) is a large igneous belt bordering the SW domain of the Ossa Morena Zone (OMZ) in Portugal (Fig. 1). It comprises three major units; 1) the Beja Layered Gabbroic Sequence (LGS) composed of a wide spectrum of olivine gabbros, rimmed by heterogeneous diorites resulting from crustal contamination and/or magma mixing processes; 2) the Cuba-Alvito Complex, mainly consisting of gabbro to (grano-)diorite; and 3) the Baleizão Porphyry Complex, a late, shallow intrusion comprising granitoid porphyritic rocks (Andrade 1983, Santos *et al*. 1990).

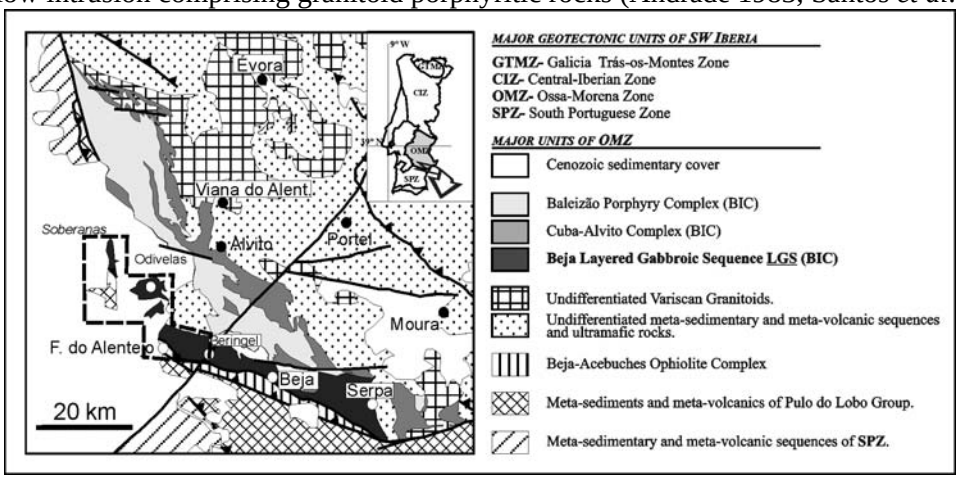

Figure 1: Location of BIC with indication of the mapped area.

Detailed mapping of LGS, between Soberanas and Beringel (see insert in Fig. 1), complemented with appropriate petrological and geochemical data, allowed the recognition of three different mineralization types: 1) Fe-Ti-V oxide, massive accumulations, 2) intercummulus Ni-Cu-Co(-PGE)

massive sulphides; and 3) late Cu(-Ni) sulphide veins. This work reports petrographic and mineral chemistry that was gathered in order to access the variation of intensive parameters throughout the evolution of the NW domain of the LGS. The results provide new insights into the genesis of the Fe-Ti-V oxide accumulations occurring at Odivelas.

2. Characterization of the NW domain of the LGS

The LGS displays NW magmatic layering dipping ~30º SW accompanied by well-developed magmatic lamination. Field and geochemical criteria indicate that the intrusion has normal polarity, supporting cartographic grouping of several gabbroic suites as Series. The NW domain of the LGS includes five Series, from North to South: Soberanas I and II (SB I and II) and Odivelas I, II and III (ODV I, II, and III). This work focus on the Series that are closely related with oxide mineralizations; therefore, excluding ODV III. SB I is a heterogeneous suite of gabbroic facies dominated by (leuco-) troctolite with coronitic coarse-grained texture (≤ 2cm, *Opx-Cpx-Hbl* rims on *Ol*) including accessory $(Spl\text{-}Chr)_{ss}$ ± Mg-rich *Ilm*. Cumulate processes account for the gradation from troctolite to lenses of fine-grained wehrlite. Minor anorthosite with poikilitic *Cpx* ± *Hbl*, microgabbro (sometimes as centimetric dikes), and pegmatoid late segregations also occur within SB I. Series SB I and SBII contact through a WNW-ESE shear zone. SB II comprises fine-grained (leuco-) norite and leucogabbro with significant amounts of intercummulus V- rich Ti-*Mgt* + *Ilm*. The transition to ODV I is covered by Cenozoic sediments. ODV I was further divided into three Groups on the basis of their mineralogical features. ODV I mainly comprises layered olivine leucogabbro that includes abundant vanadiferous Ti-*Mgt* + *Ilm* intercummulus enrichment, leading to the development of massive ores (embedded in the cumulated lenses) at the base of the Lower Group. The early accumulated $(Usp\text{-}Mgt)_{ss}$ + *Ilm* masses (< 50 t) experienced late magmatic full oxidation and re-crystallization to Ti-*Mgh* + *Ilm* (Jesus *et al.* 2003). Thick anorthosite levels are widespread in ODV I Intermediate Group. ODV I and II grade towards each other from North to South. ODV II is a rhythmic succession of olivine leucogabro and olivine gabbro where conspicuous layering and oxide occurrences are locally observed. Discontinuous anorthosite lenses characterize the uppermost levels of ODV II.

3. Modelling of intensive variables: calculation methods and restrictions

Intrusive rocks, particularly cumulate that experience long term cooling, are characterized by extensive subsolidus mineral re-equilibria that can account for pronounced compositional resetting. To minimize such effects, the most primitive mineral composition (*e.g Ol* %Fo) in each sample was selected for calculations, as they should be the closest representatives of the original conditions. Oxide phases displaying oxidation-induced exsolutions were also avoided, as these features indicate strong compositional resetting at subsolidus temperatures. Table 1 summarizes the results of the thermodynamic modelling at a constant pressure of 2 kbar; Figure 2 displays those variations throughout the studied stratigraphic succession.

The solution models embedded in *Px-QUILF* software (Andersen *et al*., 1993, and references therein) were used to calculate silicate equilibrium temperatures on the basis of the *Cpx-Opx* geothermometer. In order to compare fO_2 values obtained by distinct calculation methods, absolute fO_2 was normalized to the FMQ buffer: DFMQ ($\equiv \Delta\log(fO_2)_{FMQ} = \log (fO_2)_{sample} - \log (fO_2)_{FMQ.}$), which is insensitive to errors in T and P estimates (± 0.03 log units for ± 100 ºC or ± 10 kbar). fO_2 estimates for the crystallization of $(Chr–Spl)_{ss}$ spinels were made using Balhaus *et al.* (1991) *Spl-Ol-Opx* oxygen barometer. Although Al-Cr spinel grains do not show (oxy-)exsolution textures or significant compositional zoning, T-fO_2 estimates may be affected by spinel Fe-Mg exchange with *Ol*. fO_2 values obtained at high T (1100 ºC) appear almost invariant relative to those obtained at the closure temperatures of the mineral assemblage; thus, it is reasonable to admit that these rocks underwent cooling in a system that was buffered along a T-fO_2 path parallel to that of FMQ buffer. Equilibrium temperatures for $(Usp\text{-}Mgt)_{ss}$ + *Ilm* pairs in rocks of the more evolved Series were obtained using the modified Anderson and Lindsley thermometer (to incorporate Mg and Mn as in *Px-QUILF*). There is no overlap between calculated closure temperatures for oxides and coexisting silicates; the results indicate that strong subsolidus re-equilibrium affected the oxides, preventing the use of co-existing silicates to estimate fO_2. In these cases, fO_2 were obtained at oxide equilibrium temperature by using the reaction: 4 Fe_3O_4 (*Mgt*) + O_2 = 6Fe_2O_3 (*Hem* in *Ilm*). Assuming closed

system cooling, DFMQ estimates should be nearly equivalent to those that prevailed during the initial oxide-silicate crystallization. Estimating silica activity ($a\mathrm{SiO_2}$) by displacing the FMQ buffer to the appropriate T and $f\mathrm{O_2}$ is precluded for rocks displaying lack of equilibrium between oxides and silicates. In order to circumvent that restriction and to present homogenous results for all Series, $a\mathrm{SiO_2}$ estimates where made using the pair *Ol+Opx* following the equilibrium: $(\mathrm{Fe, Mg})_2\mathrm{Si_2O_6}$ (*Opx*)= $(\mathrm{Fe, Mg})_2\mathrm{SiO_4}$(*Ol*) + $\mathrm{SiO_2}$ (melt) at T(*Cpx-Opx*) and high T (SB I: 1200 ºC; other Series: 1100 ºC).

4. Discussion and conclusions

SB I crystallized from an oxidized (DFMQ = +2.7) primitive magma that can be considered as the LGS parental magma. The highly heterogeneous lithologic character and low silicate closure temperatures relative to other Series, suggest disturbance by successively more evolved magma batches that should account for the development of *Opx* coronas on high-Ni *Ol* grains, then rimmed by *Cpx-Hbl*. The transition from SB I to SB II Series is accompanied by a continuous compositional trend of the oxides from $(Spl\text{-}Chr)_{ss}$ to $(Mgt\text{-}Usp)_{ss}$, therefore not showing the common "spinel gap". Such continuum has been experimentally demonstrated to occur at relatively high oxidizing conditions, in agreement with the estimated oxidized nature of LGS primary magmas. The decrease in spinel #Cr is coupled by strong Cr depletion in *Cpx*. Therefore, early fractionation of Cr-rich *Spl* and *Cpx* (the silicate with the highest partitioning coefficient for Cr: $D^{Cpx/mest}_{Cr}$=34), soon impoverished the Cr concentration in the melt, inhibiting further crystallization of Cr-rich spinels. As the oxidized primitive magma gradually attained Ti saturation and the availability of Cr and Al decreased (the latter due to *Pl* fractionation), Cr-Al spinels gave way to the $(Mgt\text{-}Usp)_{ss}$, with Fe^{3+} and V^{3+} being increasingly incorporated in their structure. Fe^{3+} consumption in the magmatic liquid led to a sudden drop of $f\mathrm{O_2}$, clearly seen in the SBI-SB II transition. Accordingly, the lowest $f\mathrm{O_2}$ is observed for the oxide-rich cumulates occurring at the base of ODV-I Series. Those oxides show the highest closure T and consistently rare late oxy-exsolution reactions. Such features are interpreted as reflecting high modal proportion of the oxides, which essentially buffered the overall mineral assemblage and more easily retained their original composition. Following the oxide ore-forming event, a gradual recovery of $f\mathrm{O_2}$ is observed, resulting in DFMQ values of 0 ± 1. Massive Fe-fractionation during the initial stages of oxide-rich cumulate rocks crystallization should account for the transiently higher Fo contents in *Ol*, indicating relative Mg increase in the melt; this is followed by a "normal" fractionation trend towards Mg depletion, towards the top of the cumulate level (Fig. 2). Much broader inflexions on Fo variation trends are observed at the cumulate/ol leucogabbro transition (within ODV I) and, particularly, at the contact between ODV I and ODV II series (Fig. 2), being congruent with similar inflexions on Cr (*Cpx*) and Ni (*Ol*) concentrations. These geochemical breaks are better explained by magma recycling (variable recharge/crystallization rates), reflecting a complex evolution that should have involved repeated "primitive magma" influxes into the magma chamber(s).

Acknowledgements: The authors acknowledge the financial support of Centro de Geologia-FCUL and CREMINER. Ana Jesus acknowledges a PhD Grant SFRH/BD/6355/2001.

References

Andersen, D.J., Lindsley, D.H., Davidson, P.M., 1993. QUILF: A pascal program to assess equilibria among Fe-Mg-Mn-Ti oxides, pyroxenes, olivine, and quartz. Comp. & Geosc. 19(9), 1333-1350.

Andrade, A.S., 1983. Contribuition à l'analyse de la suture Hercynièn ne de Beja (Portugal), perspectives metallogéniques. Ph.D. thesis, INLP, University of Nancy, France.

Balhaus, C., Berry, R.F., Green, D.H., 1991. High pressure experimental calibration of the olivine-orthopyroxene-spinel oxygen geobarometer: implications for the oxidation state of the upper mantle. Contrib. Mineral. Petrol. 107, 27-40.

Jesus, A.P., 2002. Mineralizações de Fe-Ti-V e ocorrências sulfuretadas em rochas gabróicas do Complexo ígneo de Beja (Odivelas-Ferreira do Alentejo). Tese MSc, Fac. Ciênc. Univ. Lisboa.

Jesus, A.P., Mateus, A., Waerenborgh, J.C., Figueiras, J., Cerqueira, L., Oliveira, V., 2003. Massive aggregates of vanadiferous titano-maghemites in layered gabbroic rocks of the Beja Igneous Complex (Odivelas, Portugal)Hypogene titanian, vanadian maghemite in reworked oxide cumulates in the Beja Layered Gabbro Complex, Odivelas, Southeastern Portugal. Canad. Min. 41, 1105-1124.

Santos, J.F., Andrade, S.A., Munhá J., 1990. Magmatismo orogénico Varisco no limite meridional da Zona de Ossa Morena. Comun. Serv. Geol. Portugal. 76, 91-124.

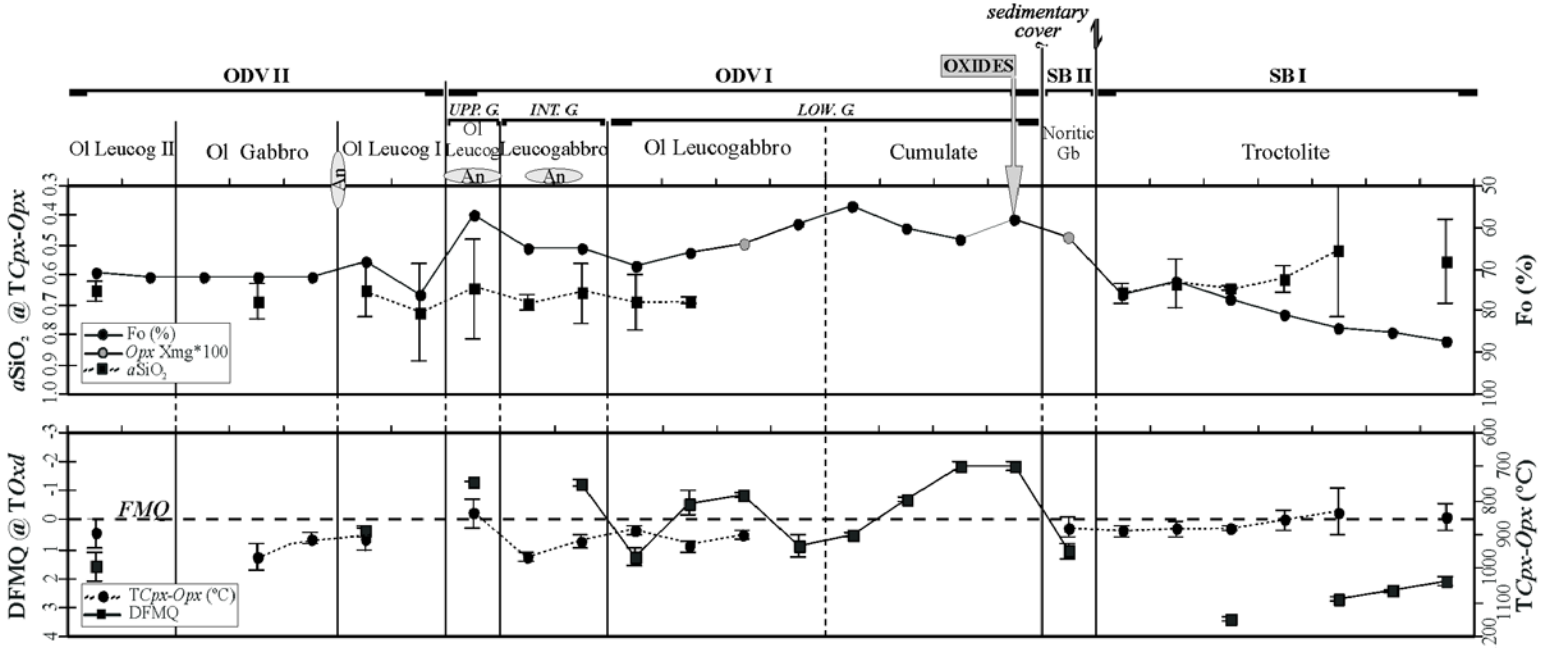

Figure 2- Variation of intensive parameters along the stratigraphic succession of the gabbroic facies as shown in the synthetic log at the left; abbreviations as in table 1. A- $aSiO_2$@T *Cpx-Opx vs Ol* %Fo ; XMg of *Opx* in rocks without *Ol* is plotted for better clearance on the sequence evolution. B- DFMQ @ TO*xd vs* T*Cpx-Opx*.

A

	EPMA Data							Thermodinamic estimates		
	Pl	*Cpx*			*Opx*	*Ol*		T*Cpx-Opx* (°C)	*a*SiO2 @ T*Cpx-Opx*	*a*SiO2 @ T*high*
	An (%)	En (%)	Wo (%)	Cr (ppm)	XMg	Fo (%)	Ni (ppm)			
SB I	76	46	46	2462	0.82	80	801	864 +/- 31	0.6 +/- 0.09	0.78 +/- 0.24
	(89-63)	(49-42)	(48-42)	(6785-1)	(0.88-0.76)	(88-73)	(2218-1)	(888-833)	(0.66-0.52)	(0.82-0.71)
	n=39		*n=27*		*n=23*	*n=33*		*N=6*	*N=6*	
SB II	65	41	44	135	0.64	-	-	878 +/- 29	-	-
	(80-50)	(42-41)	(45-43)	(289-1)	(0.65-0.63)					
	n=4		*n=5*		*n=9*			*N=1*		
ODV I	50	41	43	129	0.68	61	61	908 +/- 19	0.67 +/- 0.08	0.77 +/- 0.11
	(61-45)	(45-32)	(49-37)	(688-0)	(0.74-0.64)	(69-54)	(530-0)	(966-838)	(0.69-0.65)	(0.80-0.75)
	n=94		*n=99*		*n=18*	*n=59*		*N=5*	*N=5*	
ODV II	62	43	45	849	0.76	72	432	922 +/- 32	0.68 +/- 0.09	0.75 +/- 0.16
	(58-78)	(45-41)	(47-42)	(2937-1)	(0.77-0.74)	(77-68)	(1000-1)	(968-896)	(0.73-0.65)	(0.82-0.68)
	n=40		*n=25*		*n=15*	*n=39*		*N=4*	*N=4*	

B

	EPMA data					Thermodinamic estimates	
	Spl s.l.			*Ilm*		**(Chr-Spl)ss-Ol-Opx (Usp-Mgt)ss-(Ilm-Hem)ss*	
	# Cr/ *Cr a.p.u.f	#Mg	Usp	Hem (%)	Gk (%)	T*Oxd* (°C)	DFMQ @ T*Oxd*
SB I	0.62	0.31	0.23	3	3	*790 +/- 38	*(+2.7) +/- 0.1
	(0.69-0.54)	(0.48-0.10)	(0.34-0.15)	(8-0)	(10-0)	(838-742)	[(+3.4) - (+2.1)]
		n=17		*n=12*		*N=4*	
SB II	*0.24	0.02	0.38	6	1	601 +/- 44	(-1.1) +/- 0.2
	(0.28-0.11)	(0.03-0.01)	(0.42-0.36)				
		n=5		*n=1*		*N=1*	
ODV I	*0.03	0.03	0.46	3	2	639 +/- 40	(-0.6) +/- 0.2
	(0.24-0.00)	(0.09-0.00)	(0.84-0.34)	(8-0)	(7-0)	(814-504)	[(+1.3) - (-1.9)]
		n=83		*n=85*		*N=10*	
ODV II	*0.03	0.04	0.39	4	4	589 +/- 60	(+1) +/- 0.4
	(0.05-0.01)	(0.06-0.01)	(0.44-0.34)	(7-3)	(5-3)	(667-511)	[(+1.6) - (+0.4)]
		n=5		*n=8*		*N=2*	

Table 1- EPMA data and thermodynamic estimates for silicate (A) and oxide (B) assemblages of the studied Series; *n*= number of analyses; *N*= number of selected rock samples; @: "at" A- EPMA data and estimates obtained using *Px-QUILF* (SB I T*high*= 1200ºC;other Series T*high*= 1100ºC based on *Ol* %Fo). B-EPMA data: #Cr or Cr atoms per unit formula (based on 32 O) for $(Chr\text{-}Spl)_{ss}$ and $(Usp\text{-}Mgt)_{ss}$, spinels, respectively; #Mg and Usp of spinel *s.l.*; Hematite (% Hem) and Geikielite (% Gk) molecular contents in *Ilm*. Estimates obtained using *Px-QUILF* for $(Usp\text{-}Mgt)_{ss}$- *Ilm* or the **Spl-Ol-Opx* oxygen barometer for $(Chr\text{-}Spl)_{ss}$ spinels